

Appendix A A Medical Time Series Example

Here we use EEG data of Alzheimer's as an example. An EEG dataset has many patients with or without Alzheimer's (healthy control). Data collectors take multiple trials on a specific patient. These trials could be collected continuously within a short time or across a long period but follow the same experiment manner. Usually, the timestamps are too long for the deep learning pipeline to learn. For example, a 5 minutes trial with a sampling rate 256Hz has 76800 timestamps. Researchers generally use data preprocessing to split a trial into many samples, such as 1-second and 3-second short samples, for further representation learning. Each observation denotes a scalar or a vector of real value at a specific timestamp. An experiment with a sampling rate 256Hz has 256 observations in one second.

Appendix B Data Augmentation Banks

Binomial masking: Generate a mask following a binomial distribution that masks some timestamps of a sample, setting all channels at the masked timestamps to zero.

Channel binomial masking: Generate a mask following a binomial distribution that masks some channels of some timestamps of a sample, setting only a subset of channels at the masked timestamps to zero.

Continuous masking: Mask some continuous sequences of timestamps of a sample, setting all channels at the masked timestamps to zero.

Channel continuous masking: Mask some continuous sequences of timestamps of a sample, setting only a random half of the channels at the masked timestamps to zero.

All true: Do not apply any masking to the sample. Output the raw sample.

Appendix C Shuffle Function Banks

In real-world scenarios, ensuring the presence of samples from the same trial or patient within a training batch becomes increasingly low probability as the number of patients grows. This situation can hinder learning meaningful representations at the trial and patient levels. To address this situation, we have designed two distinct shuffle functions that serve to rearrange samples while also upholding the requirement to include samples originating from the same trial and patient. These functions are called the "trial shuffle" and the "batch shuffle".

Trial shuffle: This function shuffles samples originating from the same trial and subsequently shuffles the trial order. Initially, we arrange the samples by sorting them based on their trial IDs. Next, samples from the same trial are grouped into sets, and the order of samples within each trial set is shuffled. Finally, we sort the trial sets themselves while preserving the order of samples within each respective trial set.

Batch shuffle: This function shuffles samples in a batch and subsequently shuffles the order of batches. The logic of trial and batch shuffle are similar. Initially, we arrange the samples by sorting them based on their trial IDs. Next, we group samples into batch sets, and the order of samples within each batch set is shuffled. Finally, we sort the batch sets themselves while preserving the order of samples within each respective batch set.

Random shuffle: Besides the two specifically designed shuffle functions, this random shuffle function shuffles all the samples in the dataset.

All the shuffle functions mentioned here are designed to shuffle samples within the dataset before training. During training, it is also essential to shuffle samples each epoch to prevent the model from memorizing the dataset and encourage it to learn more useful representations. To address this, we implemented a specially crafted BatchSampler class in PyTorch, following the "batch shuffle" approach. This BatchSampler shuffles the samples locally within each epoch, ensuring that the pre-shuffled sample order is not disrupted significantly. This approach guarantees that each batch contains samples from the same trial. It's worth noting that when a batch consists of samples from the same trial, it also has samples from the same patient.

Appendix D Data Preprocessing

D.1 AD Data Preprocessing

The AD dataset [44] comprises EEG recordings from 12 patients with Alzheimer’s disease and 11 healthy controls. Each patient has an average of 30.0 ± 12.5 trials. Each trial corresponds to a 5-second interval with 1280 timestamps (sampled at 256Hz) and includes 16 channels. Prior to further processing, each trial is scaled using a standard scaler. To facilitate analysis, we segment each trial into nine half-overlapping samples, where each sample has a duration of 256 timestamps (equivalent to 1 second). Additionally, we assign a unique trial ID and patient ID to each sample based on its origin in terms of the patient and trial. We split training, validation, and test sets in a patient-independent way. We use samples from patient IDs 17 and 18 as the validation set and samples from IDs 19 and 20 as the test set. The rest of the samples are all put into the training set.

D.2 PTB Data Preprocessing

The PTB dataset [45] consists of ECG recordings from 290 patients, with 15 channels sampled at 1000 Hz. There are a total of 8 types of heart diseases present in the dataset. For this paper, we focus on binary classification using a subset of the dataset that includes 198 patients with major disease labels, specifically Myocardial infarction and healthy controls. To preprocess the ECG signals, they are first normalized using a standard scaler after being resampled to a frequency of 250 Hz. Due to special peak information in ECG signals, a regular sliding window segmentation approach may result in the loss of crucial information. To address this issue, a different segmentation strategy is employed. Instead of sliding windows, the raw trials are segmented into individual heartbeats, with each heartbeat treated as a sample. To perform this segmentation, (1) the first step involves determining the maximum duration. The median value of R-Peak intervals across all channels is calculated for each raw trial, and outliers are removed to obtain a reasonable maximum interval as the standard heartbeat duration. (2) The next step is to determine the position of the first R-Peak. The median value of the first R-Peak position is calculated and used for all channels. (3) Next, the raw trials are split into individual heartbeat segments based on the median value of their respective R-Peak intervals. Each heartbeat is sampled starting from the R-Peak position, with the segments extending to both ends with half the length of the median interval. (4) To ensure the same length of the heartbeat samples, zero padding is applied to align their lengths with the maximum duration. (5) Finally, the samples are merged into trials, where 10 nearby samples are grouped together to form a pseudo-trial, similar to the neighborhood idea presented in [17]. We split training, validation, and test sets in a patient-independent way. We use samples from 28 patients(7 healthy and 21 positive) as the validation set and samples from another 28 patients(7 healthy and 21 positive) as the test set. The rest of the samples are all put into the training set.

D.3 TDBrain Data Preprocessing

The TDBrain [46] is a large dataset that monitors the brain signals of 1274 patients with 33 channels (500 Hz) during EC (Eye closed) and EO (Eye open) tasks. The dataset consists of 60 types of diseases, and it is possible for a patient to have multiple diseases simultaneously. This paper focuses on a subset of the dataset, specifically 25 patients with Parkinson’s disease and 25 healthy controls. Only the EC task trials are used for representation learning. To process the raw EC trials, we employ a sliding window approach that continuously moves from the middle of the trial to both ends without any overlap. Each raw EC trial is divided into processed pseudo-trials with a length of 2560 timestamps (10 seconds) after resampling to 256 Hz. These processed pseudo-trials are then scaled using a standard scaler. Furthermore, each pseudo-trial is split into 19 half-overlapping samples, with each sample having a length of 256 timestamps (1 second). In addition to the binary label indicating Parkinson’s disease or healthy, each sample is assigned a patient and trial ID based on the patient and processed trial it originates from. It is important to note that the trial ID refers to the ID of the processed pseudo-trial and not the raw EC trial. We split training, validation, and test sets in a patient-independent way. We use samples from 8 patients(4 healthy and 4 positive) as the validation set and samples from another 8 patients(4 healthy and 4 positive) as the test set. The rest of the samples are all put into the training set.

Appendix E COMET and Baseline Implementation Details

We implement the baselines following their corresponding papers, including TS2vec [13], Mixing-up [16], TS-TCC [27], SimCLR [43], CLOCS [15], and TF-C [26]. In our COMET framework and all baselines, we use the last epoch of the contrastive pre-training encoder G for downstream tasks. For the P-FT and F-FT tasks, we save the best model in terms of F1 score on the validation set during training and load the saved model to evaluate the performance on the test set.

COMET (our model) We use a two-layer, fully connected network as the projection head to map the input dimension to the output dimension. The input dimension corresponds to the feature dimension of the data, while the hidden dimension is set to 128, and the output dimension is set to 64. To augment the data, we apply time series masking on the output dimension using the [all_true, all_true, continuous, continuous] (see B) for the observation, sample, trial, and patient-level contrastive blocks, respectively. The augmented output dimension from the projection head is then passed to the encoder G for representation learning. For the encoder G , we adopt a dilated CNN module. It consists of 10 hidden blocks, each following the order "GELU -> DilatedConv -> GELU -> DilatedConv." A residual connection is applied between the beginning and end of each block. The dilation factor of the convolution in the i -th block is set to 2^i . Each hidden dimension of the dilated convolution is set to 64, and the kernel size is set to 3. The output dimension of encoder G is fixed at 320. We utilize positive pair selection strategies specific to each contrastive block to build the contrastive loss in the embedding space (after encoder G). A max-pooling layer is employed before applying the representation to downstream tasks. During contrastive pre-training, we set the learning rate to 0.0001. The pre-training batch size is 256, and the total number of pre-training epochs is 100. We report the hyperparameters that achieved good results and stability among random seeds. The hyperparameters $\lambda_1, \lambda_2, \lambda_3, \lambda_4$ are assigned values of (0.25, 0.25, 0.25, 0.25), (0.1, 0.7, 0.1, 0.1), and (0.25, 0.25, 0.25, 0.25) for the AD, PTB, and TDBrain datasets, respectively.

TS2vec [13] introduces contextual consistency using overlapping subseries and a hierarchical loss function to capture data consistency at the observation and sample levels. To incorporate their methodology, we utilize the open-source code available at <https://github.com/yuezhihan/ts2vec>. However, their code does not include downstream tasks for F-FT (Full Fine-Tuning), so we implement these tasks using the same setup as our COMET. Specifically, we set the number of epochs for contrastive pre-training to 100, the learning rate to 0.0001, and the batch size to 256. To align with our model, we adjust the convolution blocks to 10, matching our configuration. We adopt the default settings provided by the TS2vec implementation for other settings during pre-training.

TS-TCC [27] leverages temporal and contextual consistency by contrasting a strong and weak augmentation. They employ a transformer-based autoregressive as the encoder. They perform a cross-view prediction by using temporal context to predict one view's future. Then, they maximize the similarity of contexts generated by the encoder to leverage contextual consistency. We utilize the open-source code available <https://github.com/emadeldeen24/TS-TCC>. We set the number of pre-training epochs to 100. We adopt the default settings provided by the TS-TCC implementation for other settings during pre-training.

Mixing-up [16] proposes a mixing-up augmentation by mixing the proportion of two time-series samples. This augmentation involves creating an augmented sample as the convex combination of two randomly selected time-series samples from the dataset. The mixing parameter follows a beta distribution, determining the proportion of the two samples in the augmentation process. We utilize the open-source code available at <https://github.com/wickstrom/mixupcontrastivelearning> to implement Mixing-up. Although they only provide downstream tasks for F-FT, we align their method with our setups for all downstream tasks, including P-FT and F-FT. We set the number of pre-training epochs to 100, the learning rate to 0.0001, and the batch size to 256 during pre-training.

SimCLR [18] is the most classic contrastive learning framework first proposed in the CV domain. It applies data augmentation techniques to create augmented views of input samples and constructs a contrastive loss based on these views. While initially designed for images, SimCLR has also been successfully adapted to time series data, as demonstrated in previous work such as [43]. To implement SimCLR, we utilize their open-source code available at <https://github.com/iantangc/ContrastiveLearningHAR>. We set the number of pre-training epochs to 100, the learning rate to 0.0001, and the batch size to 512, aligning with their recommended settings. We use the default values provided in the SimCLR implementation for other configuration parameters during pre-training.

CLOCS [15] employs samples from the same patient as positive pairs to leverage the data invariance in ECG recordings. They make use of both temporal and spatial information for contrastive learning. To implement CLOCS, we utilized their open-source code, available at <https://github.com/danikiyasseh/CLOCS>. We incorporated their contrastive loss function to implement the Contrastive Multi-segment Coding (CMSC) mechanism described in their paper. Additionally, we modified their backbone to use TCN, which shares the same network structure as our COMET, including the configuration parameters. Specifically, we set the number of pre-training epochs to 100, the learning rate to 0.0001, and the batch size to 256.

TF-C [26] leverages the consistency between time domain and frequency domain. They assume that the time-based and frequency-based representations of the same example exhibit proximity in the time-frequency space. We utilize their open-source code available at <https://github.com/mims-harvard/TFC-pretraining> to implement TF-C. While the original method is primarily designed for transfer learning, we extend it to incorporate downstream tasks such as P-FT and F-FT in our experiments. We set the number of pre-training epochs to 100, the learning rate to 0.0001, and the batch size to 256. We use the default values provided in the TF-C implementation for other configuration parameters during pre-training.

E.1 Partial Fine-tuning

In the P-FT (Partial Fine-Tuning) setup, we introduce a classifier L on top of the pre-trained encoder G , while keeping the parameters of G fixed. Only the classifier L is fine-tuned in this setup.

In the COMET, TS2vec, and Mixing-up approaches, we utilize logistic regression from the Sklearn library to implement the classifier L . We use the default settings of Sklearn, except for setting the maximum iteration to 100,000. We employ a one-layer fully connected network as the classifier L for the TF-C method. The learning rates are specifically set to $8e-5$, $3e-5$, and $1e-4$ for the AD, PTB, and TDBrain datasets, respectively. As for TS-TCC and SimCLR, we follow their respective default settings for the partial fine-tuning phase.

E.2 Full Fine-tuning

In the F-FT (Full Fine-Tuning) setup, we introduce a classifier P on top of the pre-trained encoder G , where both the parameters of the encoder G and the classifier P are trainable. In this setup, we fine-tune both the classifier P and the encoder G . We utilize a fraction of 100%, 10%, and 1% labeled training data for fine-tuning.

In the COMET, TS2vec, and Mixing-up approaches, we set the finetune learning rate to $1e-4$. We use a batch size of 128 and perform fine-tuning for 50, 100, and 100 epochs for 100%, 10%, and 1% label fractions, respectively. The classifier P is implemented as a two-layer fully connected network with hidden dimensions 128. For TF-C, we change the hidden dimension of this two-layer fully connected network to 64. The learning rates are specifically set to $8e-5$, $3e-5$, and $1e-4$ for the AD, PTB, and TDBrain datasets, respectively. Regarding TS-TCC and SimCLR, we follow their respective default settings for the full fine-tuning phase.

Appendix F Experimental Setting

F.1 Patient-Independent Experimental Setting

This paper adopts a patient-independent setting for the train-validation-test split. In medical time series classification tasks, two common approaches to splitting the data are patient-independent and patient-dependent settings [15, S1]. Figure 3 illustrates these two settings' differences. In the patient-dependent setting, samples from the same patient can appear in both the training and testing sets, whereas in the patient-independent setting, samples from the same patient are exclusively included in either the training or testing set.

Performing patient-independent representation learning poses challenges due to the unique characteristics and different data distributions exhibited by each patient [50]. Even if two patients share the same label, the patterns within their data may differ significantly due to individual noise characteristics, potentially overshadowing the common patterns observed across patients. However, in real-world scenarios, it is essential for a model to be robust and general to perform patient-independent

representation learning. The goal is to train a model on a subset of patients with known labels and utilize it to predict other patients with unknown labels. In contrast, patient-dependent classification is usually impractical since it requires knowledge of the labels for all patients.

F.2 Pseudo-Trial Experimental Setting

For many medical time series datasets, patient information is readily available, but trial information may be absent or limited to a single trial per patient. In such cases, the question arises of effectively employing trial-level contrastive learning. The solution is straightforward. We can generate pseudo-trials rather than merely deactivating the trial-level block by setting λ to 0.

We can define groups of adjacent samples as pseudo-trials and assign them the same trial ID. In our paper, we employed ten neighboring samples as a pseudo-trial for the PTB and TDBrain datasets, and this approach yielded favorable results. This concept is akin to the approach taken by TNC [17], where close samples are defined as positive pairs.

Appendix G Ablation Study, Visualization, Additional Downstream Tasks, and Heavy Duty Baseline

G.1 Ablation Study

Ablation study of contrastive blocks We examined the effectiveness of each contrastive block and progressively incorporated each block from the observation-level to all four levels. Table 5 compares the full-level COMET model with its six variants on the AD, PTB, and TDBrain datasets. The variants are as follows: (1) **O, S, R, P**, which utilize only one level of the contrastive block. We activate that specific level by setting its λ to 1 and deactivate the other three levels by setting their λ to 0; (2) **S+O**, which combines the sample and observation-level contrastive blocks. The λ values for sample and observation levels are set equally to 0.5; (3) **R+S+O**, incorporating the trial, sample, and observation-level contrastive blocks. The λ values for these three levels are set equally to 0.33; and (4) **P+R+S+O**, representing our complete COMET method with all four levels of contrastive blocks. The λ values for the four levels are set equally to 0.25. The "Fraction" column indicates the fraction of labeled training samples used during fine-tuning.

We observed that variants **R** and **P** exhibit strong performance, achieving comparable or even outperforming the full-level COMET model **P+R+S+O** on the PTB and TDBrain datasets across different fractions of labeled data (100%, 10%, and 1%). Notably, they also perform well with a 1% fraction in the AD dataset, although they exhibit significant instability in this case. This finding suggests that adding more contrastive blocks may not necessarily improve final results. Achieving a balance in weights among different levels through λ is crucial. Nevertheless, training models at individual levels can provide insights into the importance of each level in contrastive representation learning. Furthermore, it's noteworthy that the full-level COMET model **P+R+S+O** consistently demonstrates comparable or superior results across all datasets and fractions. Importantly, we did not perform any parameter tuning here, opting to set all the λ values equally, highlighting the stability of the full-level COMET **P+R+S+O** compared to other variants.

Ablation study of hyperparameter λ We conducted an analysis to assess the impact of hyperparameter λ on the AD, PTB, and TDBrain datasets in table 6. The values of $\lambda_1, \lambda_2, \lambda_3,$ and $\lambda_4,$ from left to right, correspond to the patient, trial, sample, and observation levels, respectively. In this analysis, all four data levels are incorporated, representing the full-level COMET model **P+R+S+O**. We applied a significant weight to one data level by setting its corresponding λ to 0.7 while assigning lower weights of 0.1 to the other levels. Furthermore, we explored scenarios with increased weights on patient and trial levels or sample and observation levels. The "Fraction" column indicates the fraction of labeled training samples used during fine-tuning.

We observed that the results exhibited greater stability than the ablation study of contrastive blocks. In the contrastive block ablation study, there were significant discrepancies between different COMET variants at times. For instance, the **S** and **R** variants of the TDBrain dataset exhibited substantial differences across various fraction setups. However, in the full-level COMET model, the differences between these inter-running setups were notably reduced, even when a heavy weight was applied to one data level. For instance, the differences between lambda setups (0.1, 0.1, 0.7, 0.1) and (0.1,

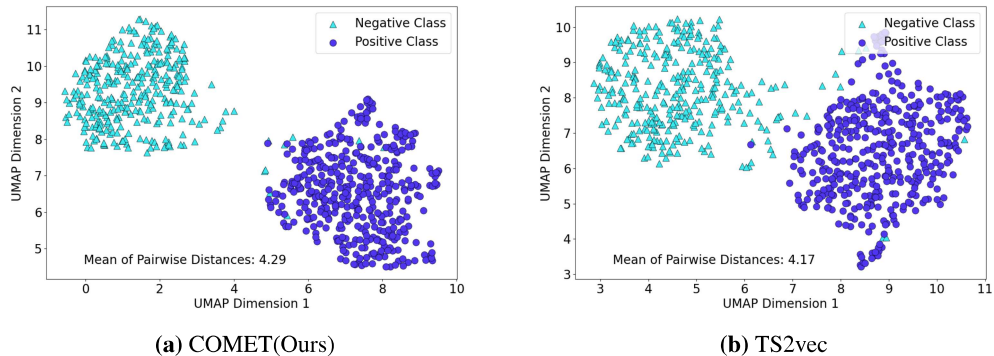


Figure 4: Visualizing the learned representation (a) Visualization for TS2vec. (b) Visualization for COMET(Ours). The visualized representation is trained in the F-FT setup on the AD dataset. Dark blue and light blue denotes the negative class(Health) and positive class(Alzheimer), respectively. We calculate the mean Euclidean distance between pairwise samples from two classes for each pair of samples to evaluate the class separability. As the figure shows, our method exhibits superior separation between the two classes, resulting in larger pairwise distances.

0.7, 0.1, 0.1) were not as significant in the TDBrain dataset. This observation underscores again the stability and robustness of the full-level COMET model.

G.2 Visualization

To visualize the effectiveness of COMET, we depict the learned representation h_i using the F-FT setup on the AD dataset as a case study. It is important to note that the learned representation h_i consists of 320 dimensions after pooling. To visualize the representations more interpretably, we employ UMAP, a dimensionality reduction technique with 20 neighbors and a minimum distance of 0.2. To establish a benchmark for comparison, we utilize TS2vec, which has shown the best performance among all baselines in the F-FT setup on the AD dataset. Additionally, we compute the average pairwise Euclidean distance between the negative (healthy) and positive (Alzheimer) classes, offering a quantitative measure of separability between the two classes.

G.3 Performance on Downstream Tasks

Clustering We assess the clustering performance of COMET using the AD dataset as a case study. Instead of employing a classifier model on top of the encoder, we apply K-means clustering ($K=2$) to the encoder G . We utilize three widely-used evaluation metrics: Silhouette score, Adjusted Rand Index (ARI), and Normalized Mutual Information (NMI). To establish a benchmark for comparison, we consider TS2vec, which has shown the best performance among all baselines in the F-FT setup on the AD dataset. Table 7 illustrates that COMET surpasses TS2vec with an improvement of 0.0586 in Silhouette score, 0.945 in ARI, and 0.881 in NMI.

Anomaly detection We evaluate the anomaly detection performance of COMET using the AD dataset as a case study. While some previous works focus on identifying outlier observations within a sample [S2, S3], we concentrate on sample-level anomaly detection. We construct a very unbalanced AD test set comprising 90% negative (healthy) samples and 10% positive (Alzheimer’s) samples. The negative samples are considered normal, while the positive samples are treated as outliers. The test set is prepared accordingly, while the remaining aspects of the experiment follow the F-FT setup. Specifically, We utilize the saved trained models from the F-FT setup to evaluate the new test set, and for comparison, we still employ TS2vec as a benchmark. The "Fraction" column indicates the fraction of labeled training samples used during fine-tuning. The experiment result is shown in table 8. The COMET outperforms TS2vec by 5.25%, 15.3% and 11.4% with label fraction 100%, 10% and 1%, respectively.

Table 5: Ablation study of contrastive blocks. The ablation study of contrastive blocks is evaluated on the AD, TDBrain, and PTB datasets. We examine the effectiveness of each contrastive block. Besides, we progressively incorporate each block from the observation-level to all four levels. Here, **O**, **S**, **R**, and **P** denote the observation, sample, trial, and patient-level contrastive blocks, respectively.

Datasets	Fraction	Blocks	Accuracy	Precision	Recall	F1 score	AUROC	AUPRC
AD	100%	O	81.69±10.71	87.28±5.71	79.64±12.07	78.90±13.78	92.54±4.18	92.36±4.34
		S	83.53±2.89	84.35±1.69	82.81±3.56	82.97±3.47	91.01±1.96	90.81±1.95
		R	78.58±14.99	83.14±11.60	76.31±16.66	74.53±18.69	85.05±12.74	84.44±13.22
		P	72.69±13.13	78.67±11.81	69.74±14.50	67.04±17.27	83.30±13.91	82.57±14.29
		S+O	85.70±1.82	86.14±1.63	85.09±2.04	85.35±1.96	92.21±1.40	92.09±1.39
		R+S+O	85.57±4.04	88.12±2.58	84.31±4.79	84.73±4.59	93.28±2.52	92.98±2.83
		P+R+S+O	84.50±4.46	88.31±2.42	82.95±5.39	83.33±5.15	94.44±2.37	94.43±2.48
	10%	O	86.35±9.25	87.09±9.04	85.55±9.92	85.70±10.10	92.62±8.99	92.77±8.72
		S	77.30±3.63	78.45±3.75	76.26±3.91	76.36±3.92	85.43±3.61	84.63±3.76
		R	77.83±17.59	83.45±14.35	75.41±19.62	72.08±23.45	83.51±16.90	83.27±17.00
		P	71.41±15.31	76.91±15.56	68.70±16.46	66.54±17.74	76.11±16.98	76.06±16.19
		S+O	82.73±2.05	84.33±2.71	81.51±2.07	81.98±2.11	90.02±2.47	90.02±2.40
		R+S+O	91.19±3.14	91.74±3.01	90.70±3.34	90.98±3.25	95.86±2.63	95.86±2.67
		P+R+S+O	91.43±3.12	92.52±2.36	90.71±3.56	91.14±3.31	96.44±2.84	96.48±2.82
	1%	O	69.56±7.54	71.43±8.04	68.19±7.16	67.83±7.41	77.32±8.69	77.32±8.45
		S	59.09±3.50	61.08±4.86	59.83±4.00	58.12±3.57	63.99±6.62	63.33±6.09
		R	90.15±13.23	93.83±7.28	89.03±14.88	88.17±16.78	96.22±5.97	96.02±6.28
		P	85.57±13.45	90.36±7.16	83.98±15.13	82.72±18.03	94.23±5.82	94.10±5.65
		S+O	63.24±3.62	63.52±4.15	63.30±4.26	62.72±4.14	67.98±5.17	67.25±4.97
		R+S+O	82.65±4.23	83.21±4.06	82.97±4.58	82.46±4.43	90.07±6.77	90.24±6.56
		P+R+S+O	88.22±3.36	88.55±2.73	88.56±3.14	88.14±3.37	96.05±1.37	96.12±1.31
	100%	O	85.27±1.73	84.21±1.25	77.74±4.01	79.78±3.37	88.13±2.23	84.76±2.14
		S	84.30±2.56	84.00±2.16	75.68±5.69	77.74±5.13	88.66±2.05	84.80±2.15
		R	88.63±1.43	88.42±1.45	82.46±2.35	84.72±2.12	89.29±3.96	86.21±4.96
P		88.85±3.22	88.74±2.30	82.78±6.11	84.75±5.38	94.32±1.81	90.61±2.81	
S+O		84.38±2.34	84.33±1.18	75.49±5.69	77.69±4.76	90.37±2.59	86.57±4.32	
R+S+O		85.32±1.93	84.82±1.78	77.54±4.58	79.64±3.94	92.34±1.85	88.75±1.98	
P+R+S+O		86.36±1.44	87.18±1.28	77.87±2.55	80.79±2.44	93.41±2.35	89.09±1.64	
PTB	10%	O	86.75±1.44	85.42±2.10	80.88±3.27	82.45±2.29	90.71±3.16	88.84±3.59
		S	86.34±0.73	84.75±1.49	80.21±1.78	81.90±1.25	88.36±0.31	85.20±1.17
		R	88.12±1.75	86.36±2.28	84.16±3.55	84.80±2.39	91.80±2.50	90.45±1.90
		P	90.38±2.23	90.33±2.71	85.69±4.36	87.27±3.45	93.06±3.86	91.83±2.93
		S+O	85.84±1.74	84.14±0.76	80.07±5.18	81.14±3.82	90.28±2.75	87.57±3.42
		R+S+O	85.88±3.08	83.60±3.61	82.45±1.94	82.48±2.71	90.79±1.79	88.68±1.91
		P+R+S+O	90.32±1.61	89.67±1.94	85.85±2.99	87.35±2.36	92.78±1.11	90.46±3.09
1%	O	85.73±1.59	83.79±2.15	79.53±3.14	81.09±2.54	90.15±2.32	88.85±2.64	
	S	77.63±1.72	72.36±2.41	69.41±2.53	70.38±2.29	79.09±2.21	75.07±1.88	
	R	86.28±1.97	84.02±2.85	82.06±2.08	82.61±1.97	90.50±0.99	88.32±1.40	
	P	91.55±2.45	90.28±3.27	88.45±3.22	89.25±3.13	95.12±2.58	94.80±2.04	
	S+O	81.78±1.07	77.65±1.34	77.17±2.14	77.20±1.43	86.65±2.38	82.12±1.95	
	R+S+O	80.71±2.28	76.79±2.03	80.51±1.67	77.84±2.13	88.76±1.38	85.00±2.23	
	P+R+S+O	86.62±3.90	82.99±4.52	85.36±5.73	83.89±4.96	93.78±3.82	91.94±4.96	
100%	O	89.92±2.15	90.50±2.07	89.92±2.15	89.89±2.17	96.79±1.29	96.84±1.29	
	S	77.86±2.85	78.98±2.51	77.86±2.85	77.62±3.01	88.44±2.23	88.96±2.14	
	R	94.44±1.79	94.60±1.75	94.44±1.79	94.44±1.80	98.39±1.29	98.31±1.46	
	P	93.18±3.70	93.27±3.67	93.18±3.70	93.18±3.70	97.59±2.01	97.58±2.00	
	S+O	80.38±4.22	81.59±3.70	80.38±4.22	80.16±4.38	91.35±2.24	91.64±2.05	
	R+S+O	86.01±4.29	86.35±3.81	86.01±4.29	85.95±4.38	94.14±2.72	94.37±2.58	
	P+R+S+O	85.47±1.16	85.68±1.20	85.47±1.16	85.45±1.16	93.73±1.02	93.96±0.99	
TDBrain	10%	O	85.34±4.38	86.03±3.97	85.34±4.38	85.25±4.48	93.18±3.52	93.24±3.53
		S	74.02±2.09	74.62±2.01	74.02±2.09	73.86±2.17	81.92±3.25	81.76±3.42
		R	92.96±8.22	93.02±8.20	92.96±8.22	92.96±8.23	96.14±5.80	95.93±6.08
		P	89.38±14.69	89.58±14.72	89.38±14.69	89.36±14.69	93.23±11.81	93.52±11.10
		S+O	74.92±2.57	76.60±3.07	74.92±2.57	74.54±2.55	84.51±3.07	84.40±3.07
		R+S+O	81.90±4.74	83.55±4.02	81.90±4.74	81.61±4.99	91.21±3.52	90.73±3.72
		P+R+S+O	79.28±4.64	79.83±4.83	79.28±4.64	79.19±4.62	88.39±4.13	88.38±3.96
1%	O	71.52±7.54	72.17±7.71	71.52±7.54	71.31±7.62	78.32±8.37	77.56±8.91	
	S	58.62±3.84	59.66±3.95	58.62±3.84	57.39±4.26	62.85±6.38	61.61±6.61	
	R	85.29±5.93	85.55±5.66	85.29±5.93	85.24±5.99	91.19±4.76	91.11±4.74	
	P	77.23±3.42	78.10±3.39	77.23±3.42	77.04±3.47	86.12±3.88	85.10±4.11	
	S+O	61.71±2.97	61.82±2.90	61.71±2.97	61.60±3.07	66.09±2.98	64.94±2.66	
	R+S+O	72.15±6.26	73.39±7.50	72.15±6.26	71.91±6.12	78.39±7.77	76.97±7.61	
	P+R+S+O	72.93±7.21	74.20±7.68	72.93±7.21	72.57±7.37	78.72±8.42	77.71±9.10	

Table 6: Ablation study of hyperparameter λ . The ablation study of hyperparameter λ is evaluated on the AD, TDBrain, and PTB datasets. The $\lambda_1, \lambda_2, \lambda_3, \lambda_4$ from left to right are for patient, trial, sample, and observation levels, respectively.

Datasets	Fraction	$\lambda_1, \lambda_2, \lambda_3, \lambda_4$	Accuracy	Precision	Recall	F1 score	AUROC	AUPRC	
AD	100%	(0.1,0.1,0.1,0.7)	87.82\pm7.44	91.08\pm4.10	86.62\pm8.58	86.77\pm8.64	97.95\pm1.26	97.94\pm1.26	
		(0.1,0.1,0.7,0.1)	85.03 \pm 5.64	89.09 \pm 3.22	83.32 \pm 6.37	83.78 \pm 6.59	95.33 \pm 1.81	95.30 \pm 1.90	
		(0.1,0.7,0.1,0.1)	82.76 \pm 8.67	88.00 \pm 4.65	80.98 \pm 10.02	80.72 \pm 10.30	95.32 \pm 2.72	95.26 \pm 2.71	
		(0.7,0.1,0.1,0.1)	82.22 \pm 8.31	87.27 \pm 4.41	80.42 \pm 9.62	80.17 \pm 10.00	94.84 \pm 2.64	94.80 \pm 2.65	
		(0.2,0.2,0.3,0.3)	86.88 \pm 5.78	89.96 \pm 4.00	85.46 \pm 6.52	85.97 \pm 6.36	94.03 \pm 3.56	94.07 \pm 3.54	
		(0.3,0.3,0.2,0.2)	86.72 \pm 5.97	89.76 \pm 3.12	85.41 \pm 6.92	85.73 \pm 6.96	95.14 \pm 1.95	95.09 \pm 2.04	
	(0.3,0.3,0.15,0.25)	82.84 \pm 6.96	88.09 \pm 3.99	80.87 \pm 7.93	81.04 \pm 8.06	94.73 \pm 2.98	94.64 \pm 3.12		
	10%	(0.1,0.1,0.1,0.7)	89.56 \pm 8.67	91.37 \pm 6.73	88.64 \pm 9.65	88.82 \pm 9.51	96.55 \pm 4.41	96.47 \pm 4.63	
		(0.1,0.1,0.7,0.1)	87.84 \pm 6.09	88.72 \pm 5.16	87.50 \pm 6.76	87.42 \pm 6.66	94.58 \pm 5.32	94.38 \pm 5.67	
		(0.1,0.7,0.1,0.1)	79.89 \pm 14.06	85.79 \pm 7.50	77.97 \pm 16.05	75.54 \pm 19.81	92.89 \pm 6.45	92.67 \pm 6.64	
		(0.7,0.1,0.1,0.1)	78.26 \pm 13.58	84.99 \pm 6.68	76.38 \pm 15.80	73.44 \pm 19.24	92.74 \pm 7.64	92.57 \pm 7.93	
		(0.2,0.2,0.3,0.3)	93.25\pm1.71	93.86\pm1.24	92.77\pm2.00	93.09\pm1.80	97.68\pm0.87	97.75\pm0.82	
		(0.3,0.3,0.2,0.2)	91.43 \pm 3.70	92.71 \pm 2.39	90.68 \pm 4.28	91.09 \pm 4.00	96.81 \pm 1.62	96.88 \pm 1.62	
	(0.3,0.3,0.15,0.25)	91.54 \pm 3.63	92.93 \pm 2.32	90.77 \pm 4.25	91.19 \pm 3.91	97.26 \pm 1.63	97.29 \pm 1.67		
	1%	(0.1,0.1,0.1,0.7)	95.88 \pm 2.29	96.21 \pm 1.92	95.64 \pm 2.55	95.79 \pm 2.36	92.72 \pm 9.34	93.24 \pm 8.74	
		(0.1,0.1,0.7,0.1)	85.03 \pm 9.80	87.16 \pm 5.75	85.65 \pm 8.54	84.62 \pm 10.42	94.71 \pm 2.73	94.73 \pm 2.89	
		(0.1,0.7,0.1,0.1)	97.19\pm1.28	97.32\pm1.11	97.08\pm1.42	97.15\pm1.31	99.02\pm1.06	98.98\pm1.11	
		(0.7,0.1,0.1,0.1)	97.00 \pm 1.10	97.10 \pm 1.06	96.92 \pm 1.14	96.96 \pm 1.12	98.93 \pm 1.20	98.89 \pm 1.26	
		(0.2,0.2,0.3,0.3)	84.55 \pm 7.39	84.47 \pm 7.51	84.75 \pm 7.65	84.44 \pm 7.49	89.95 \pm 10.83	89.78 \pm 11.27	
		(0.3,0.3,0.2,0.2)	86.96 \pm 5.92	87.16 \pm 5.66	86.87 \pm 6.31	86.72 \pm 6.19	92.68 \pm 7.76	92.93 \pm 7.43	
	(0.3,0.3,0.15,0.25)	92.40 \pm 2.52	92.75 \pm 2.41	92.16 \pm 2.44	92.27 \pm 2.55	97.76 \pm 1.11	97.76 \pm 1.17		
	PTB	100%	(0.1,0.1,0.1,0.7)	85.51 \pm 2.46	85.54 \pm 2.52	76.96 \pm 4.20	79.60 \pm 3.91	91.30 \pm 2.28	87.11 \pm 3.84
			(0.1,0.1,0.7,0.1)	85.94 \pm 3.40	87.23 \pm 4.03	76.69 \pm 5.61	79.64 \pm 5.94	93.78 \pm 2.51	90.78\pm4.78
			(0.1,0.7,0.1,0.1)	87.84\pm1.98	87.67 \pm 1.72	81.14\pm3.68	83.45\pm3.22	92.95 \pm 1.56	87.47 \pm 2.82
(0.7,0.1,0.1,0.1)			87.76 \pm 2.75	88.20\pm1.41	80.65 \pm 5.54	82.96 \pm 5.07	91.82 \pm 3.66	88.70 \pm 3.08	
(0.2,0.2,0.3,0.3)			87.74 \pm 1.46	87.78 \pm 1.48	80.79 \pm 2.58	83.28 \pm 2.31	92.97 \pm 1.97	88.67 \pm 1.71	
(0.3,0.3,0.2,0.2)			87.16 \pm 2.02	87.62 \pm 1.60	79.47 \pm 3.69	82.15 \pm 3.33	94.00\pm0.42	88.83 \pm 1.65	
(0.3,0.3,0.15,0.25)		87.56 \pm 0.87	87.91 \pm 0.64	80.25 \pm 1.69	82.92 \pm 1.50	91.85 \pm 2.44	88.27 \pm 2.34		
10%		(0.1,0.1,0.1,0.7)	87.76 \pm 2.62	87.15 \pm 2.27	81.53 \pm 5.10	83.43 \pm 4.15	92.54 \pm 2.17	89.85 \pm 2.65	
		(0.1,0.1,0.7,0.1)	88.29 \pm 2.53	85.80 \pm 3.57	86.87\pm1.39	85.89 \pm 2.34	94.56 \pm 0.80	93.15\pm0.78	
		(0.1,0.7,0.1,0.1)	88.49 \pm 3.28	88.98 \pm 2.60	81.65 \pm 6.00	84.01 \pm 5.61	94.83\pm1.08	92.48 \pm 2.22	
		(0.7,0.1,0.1,0.1)	88.70 \pm 3.20	89.47\pm2.40	81.85 \pm 6.02	84.26 \pm 5.45	94.30 \pm 1.76	93.24 \pm 2.41	
		(0.2,0.2,0.3,0.3)	89.25 \pm 2.07	88.87 \pm 2.55	83.98 \pm 3.97	85.72 \pm 3.13	94.26 \pm 1.47	90.82 \pm 3.43	
	(0.3,0.3,0.2,0.2)	89.39 \pm 2.02	88.86 \pm 2.90	84.43 \pm 3.65	86.03 \pm 3.00	93.59 \pm 1.13	92.42 \pm 2.00		
(0.3,0.3,0.15,0.25)	89.82\pm3.00	89.36 \pm 2.16	84.71 \pm 5.73	86.34\pm4.84	93.55 \pm 1.96	90.54 \pm 3.20			
1%	(0.1,0.1,0.1,0.7)	89.45 \pm 1.80	87.49 \pm 2.15	86.23 \pm 3.61	86.62 \pm 2.57	94.03 \pm 2.59	93.21 \pm 2.60		
	(0.1,0.1,0.7,0.1)	85.12 \pm 2.24	81.33 \pm 2.60	83.06 \pm 3.24	82.01 \pm 2.76	91.12 \pm 2.14	88.96 \pm 2.92		
	(0.1,0.7,0.1,0.1)	90.52\pm1.90	88.58\pm2.93	88.23 \pm 1.98	88.23\pm2.10	95.08 \pm 1.50	93.78 \pm 1.98		
	(0.7,0.1,0.1,0.1)	90.19 \pm 1.75	87.88 \pm 2.23	88.20 \pm 2.70	87.87 \pm 2.19	94.82 \pm 1.65	93.68 \pm 2.24		
	(0.2,0.2,0.3,0.3)	85.28 \pm 4.39	81.48 \pm 5.03	84.10 \pm 5.66	82.47 \pm 5.28	92.87 \pm 3.85	90.34 \pm 4.96		
	(0.3,0.3,0.2,0.2)	86.96 \pm 2.56	83.38 \pm 2.89	85.65 \pm 3.59	84.32 \pm 3.15	94.47 \pm 1.90	92.31 \pm 2.67		
(0.3,0.3,0.15,0.25)	89.43 \pm 1.38	86.42 \pm 1.96	88.86\pm0.94	87.37 \pm 1.39	95.32\pm1.04	94.29\pm1.72			
PTB	100%	(0.1,0.1,0.1,0.7)	87.20 \pm 3.39	87.40 \pm 3.34	87.20 \pm 3.39	87.18 \pm 3.40	94.84 \pm 2.34	94.96 \pm 2.33	
		(0.1,0.1,0.7,0.1)	88.53\pm3.86	88.66\pm3.79	88.53\pm3.86	88.52\pm3.87	95.57 \pm 2.74	95.71 \pm 2.66	
		(0.1,0.7,0.1,0.1)	87.97 \pm 3.26	88.33 \pm 3.15	87.97 \pm 3.26	87.94 \pm 3.28	95.58\pm1.92	95.77\pm1.86	
		(0.7,0.1,0.1,0.1)	87.25 \pm 2.71	87.54 \pm 2.74	87.25 \pm 2.71	87.22 \pm 2.71	95.14 \pm 1.73	95.32 \pm 1.70	
		(0.2,0.2,0.3,0.3)	85.69 \pm 2.42	86.00 \pm 2.53	85.69 \pm 2.42	85.66 \pm 2.41	94.14 \pm 1.43	94.31 \pm 1.28	
		(0.3,0.3,0.2,0.2)	85.76 \pm 3.18	86.24 \pm 2.75	85.76 \pm 3.18	85.69 \pm 3.24	94.34 \pm 1.79	94.45 \pm 1.77	
	(0.3,0.3,0.15,0.25)	85.54 \pm 4.11	86.30 \pm 3.62	85.54 \pm 4.11	85.44 \pm 4.21	94.22 \pm 2.86	94.36 \pm 2.80		
	10%	(0.1,0.1,0.1,0.7)	76.92 \pm 4.84	78.35 \pm 3.64	76.92 \pm 4.84	76.50 \pm 5.33	85.85 \pm 3.99	85.36 \pm 4.30	
		(0.1,0.1,0.7,0.1)	81.91 \pm 5.84	82.40 \pm 5.82	81.91 \pm 5.84	81.83 \pm 5.87	90.38 \pm 5.11	90.72 \pm 5.16	
		(0.1,0.7,0.1,0.1)	84.51 \pm 4.81	84.90 \pm 4.61	84.51 \pm 4.81	84.45 \pm 4.86	92.58 \pm 3.30	92.62 \pm 3.09	
		(0.7,0.1,0.1,0.1)	84.92\pm5.83	85.24\pm5.43	84.92\pm5.83	84.86\pm5.94	92.69\pm4.07	92.69\pm3.81	
		(0.2,0.2,0.3,0.3)	80.79 \pm 3.84	82.00 \pm 3.76	80.79 \pm 3.84	80.59 \pm 3.94	89.88 \pm 3.50	89.56 \pm 3.76	
(0.3,0.3,0.2,0.2)		78.93 \pm 3.88	79.78 \pm 4.06	78.93 \pm 3.88	78.77 \pm 3.94	88.64 \pm 3.52	88.59 \pm 3.24		
(0.3,0.3,0.15,0.25)	79.96 \pm 5.63	81.00 \pm 5.52	79.96 \pm 5.63	79.76 \pm 5.76	88.89 \pm 4.57	88.70 \pm 4.21			
1%	(0.1,0.1,0.1,0.7)	68.68 \pm 2.88	70.46 \pm 3.56	68.68 \pm 2.88	68.02 \pm 2.95	73.79 \pm 4.80	72.99 \pm 5.27		
	(0.1,0.1,0.7,0.1)	66.49 \pm 8.01	68.46 \pm 7.64	66.49 \pm 8.01	65.03 \pm 9.26	73.30 \pm 8.15	72.74 \pm 8.32		
	(0.1,0.7,0.1,0.1)	73.08 \pm 8.61	74.89\pm8.18	73.08 \pm 8.61	72.45 \pm 8.89	78.39 \pm 4.58	77.79 \pm 4.18		
	(0.7,0.1,0.1,0.1)	73.16 \pm 8.72	75.14 \pm 8.13	73.16 \pm 8.72	72.46 \pm 9.05	78.42 \pm 4.48	77.76 \pm 4.05		
	(0.2,0.2,0.3,0.3)	71.55 \pm 8.49	72.14 \pm 9.14	71.55 \pm 8.49	71.44 \pm 8.44	77.14 \pm 9.24	76.04 \pm 9.79		
	(0.3,0.3,0.2,0.2)	70.11 \pm 8.07	71.68 \pm 8.95	70.11 \pm 8.07	69.54 \pm 8.38	76.24 \pm 10.55	75.26 \pm 10.84		
(0.3,0.3,0.15,0.25)	73.59\pm9.28	74.53 \pm 9.61	73.59\pm9.28	73.33\pm9.36	79.07\pm9.67	77.97\pm9.62			

Table 7: Performance on downstream clustering. The clustering performance is evaluated on the AD dataset. We compare the baseline TS2vec, which performs best in the F-FT setup.

Method	Silhouette	ARI	NMI
Random Init.	0.1184±0.0082	0.1189±0.0664	0.1258±0.0660
TS2vec	0.0795±0.0032	0.0013±0.0026	0.0018±0.0016
COMET (Ours)	0.1381±0.0139	0.9358±0.0264	0.8827±0.0414

Table 8: Performance on anomaly detection. Sample-level anomaly detection on a very unbalanced AD test set comprising 90% negative (healthy) samples and 10% positive (Alzheimer) samples.

Fraction	Models	Accuracy	Precision	Recall	F1 score	AUROC	AUPRC
100%	TS2vec	82.11±3.30	66.05±2.45	82.13±3.21	68.70±3.37	91.27±1.47	76.80±3.08
	COMET (Ours)	83.03±11.65	71.76±7.60	90.33±6.31	73.95±11.97	97.99±1.37	91.52±5.52
10%	TS2vec	76.05±6.35	62.48±2.90	77.33±4.74	62.67±5.00	86.76±3.95	72.21±5.09
	COMET (Ours)	88.22±2.88	73.22±3.31	92.49±1.73	77.97±3.87	97.91±1.14	92.21±4.43
1%	TS2vec	67.24±8.05	57.34±3.12	67.87±6.45	54.35±6.21	72.75±6.82	61.32±5.25
	COMET (Ours)	77.57±4.21	64.72±1.95	84.41±3.38	65.74±3.67	93.13±2.82	79.65±7.65

G.4 Heavy Duty Baselines

In COMET, we incorporate four contrastive blocks to leverage four levels of data consistency, allowing the data to pass through the model four times within one epoch during contrastive pre-training. To ensure that our superior performance is not due to increased data passing, we conduct experiments on the AD dataset with two baselines: SimCLR and TS2vec.

SimCLR utilizes only one contrastive block during training. We employ two strategies to match the data passing number with COMET: (1) Run SimCLR with one contrastive block for four times the original number of epochs in pre-training (400 epochs instead of 100). (2) Duplicate the contrastive blocks, resulting in four SimCLR contrastive blocks. The notation **4E** signifies running the model for four times the original number of epochs, while **4B** indicates the use of four times the number of contrastive blocks compared to the original SimCLR.

TS2vec incorporates two contrastive blocks during training, leading to data passing twice within one epoch. Similarly, we adopt two strategies to align the data passing number with COMET: (1) Run TS2vec for two times the original number of epochs in pre-training (200 epochs instead of 100). (2) Duplicate the contrastive blocks, resulting in four TS2vec contrastive blocks. The notation **2E** denotes running the model for four times the original number of epochs, while **2B** indicates the use of four times the number of contrastive blocks compared to the original TS2vec.

The results are presented in Table 9. We observe that simply increasing the number of epochs or contrastive blocks does not improve performance but rather leads to a decrease in most cases. We speculate that this decrease is caused by overfitting.

Appendix H Broader Impacts

Our approach for self-supervised contrastive learning improves classification performance on target datasets in patient-independent medical diagnosis scenarios. Leveraging different data consistency levels in medical time series is crucial to enable effective and accurate contrastive learning without sufficient labels. Our work will encourage the research community to discover universal frameworks for other practical applications based on time series representation learning. We also hope our work can attract more researchers to the more general problem of hierarchical consistency from other related fields.

From the societal perspective, our work and the line of contrastive learning can promote more efficient use of medical time series with the lack of labels. Specifically, our model has the potential to identify patterns and anomalies that may not be immediately apparent to human experts. This could lead to earlier and more accurate diagnoses, improving patient outcomes and reducing healthcare costs. However, practitioners need to be aware of the limitations of the model.

Table 9: Heavy Duty Baselines. Run more epochs or add more contrastive blocks to SimCLR and TS2vec on the AD dataset.

Fraction	Models	Accuracy	Precision	Recall	F1 score	AUROC	AUPRC
100%	4E-SimCLR	56.87±2.51	57.67±4.02	53.31±2.30	48.28±4.63	57.67±4.02	51.97±1.44
	4B-SimCLR	53.92±3.81	51.88±3.25	51.26±3.05	46.92±5.07	51.88±3.25	50.75±1.69
	SimCLR	54.77±1.97	50.15±7.02	50.58±1.92	43.18±4.27	50.15±7.02	50.42±1.06
	2E-TS2vec	76.49±6.10	78.97±3.54	77.69±5.16	76.21±6.45	88.44±2.40	88.12±2.53
	2B-TS2vec	81.61±1.65	81.47±1.75	81.53±1.68	81.43±1.65	89.50±1.60	89.22±1.75
	TS2vec	81.26±2.08	81.21±2.14	81.34±2.04	81.12±2.06	89.20±1.76	88.94±1.85
	COMET (Ours)	84.50±4.46	88.31±2.42	82.95±5.39	83.33±5.15	94.44±2.37	94.43±2.48
10%	4E-SimCLR	57.97±1.74	58.41±8.31	53.69±2.25	46.47±5.71	58.41±8.31	52.33±1.38
	4B-SimCLR	53.57±6.29	53.89±5.05	52.97±4.22	50.60±5.46	53.89±5.05	51.80±2.34
	SimCLR	56.09±2.25	53.81±5.74	51.73±2.59	44.10±4.84	53.81±5.74	51.08±1.53
	2E-TS2vec	66.29±7.86	69.92±5.13	67.79±6.44	65.36±8.55	78.54±4.98	77.95±5.29
	2B-TS2vec	72.61±4.46	73.86±4.36	72.98±3.66	72.30±4.24	81.91±4.83	81.74±4.85
	TS2vec	73.28±4.34	74.14±4.33	73.52±3.77	73.00±4.18	81.66±5.20	81.58±5.11
	COMET (Ours)	91.43±3.12	92.52±2.36	90.71±3.56	91.14±3.31	96.44±2.84	96.48±2.82
1%	4E-SimCLR	58.07±1.93	57.72±3.50	54.92±1.99	51.93±3.11	57.72±3.50	52.91±1.28
	4B-SimCLR	54.67±5.43	54.86±4.94	54.48±4.64	53.68±4.89	54.86±4.94	52.67±2.68
	SimCLR	55.42±2.43	52.18±5.55	51.37±2.76	45.02±4.79	52.18±5.55	50.87±1.45
	2E-TS2vec	63.56±4.62	64.97±3.53	64.49±3.90	63.28±4.69	70.26±3.55	68.77±3.59
	2B-TS2vec	64.18±4.53	64.26±4.80	64.26±4.80	63.93±4.61	70.07±5.97	68.62±6.25
	TS2vec	64.93±3.53	65.28±3.52	65.14±3.59	64.64±3.58	70.56±5.38	68.97±5.75
	COMET (Ours)	88.22±3.36	88.55±2.73	88.56±3.14	88.14±3.37	96.05±1.36	96.12±1.31

All datasets in this paper are publicly available and are not associated with privacy or security concerns. Furthermore, we have followed guidelines on responsible use specified by the primary authors of the datasets used in the current work.

Appendix References

- [S1] Cosimo Ieracitano, Nadia Mammone, Alessia Bramanti, Amir Hussain, and Francesco C Morabito. A convolutional neural network approach for classification of dementia stages based on 2d-spectral representation of eeg recordings. Neurocomputing, 323:96–107, 2019.
- [S2] Ling Yang and Shenda Hong. Unsupervised time-series representation learning with iterative bilinear temporal-spectral fusion. In International Conference on Machine Learning, pages 25038–25054. PMLR, 2022.
- [S3] Dennis Bäbler, Tobias Kortus, and Gabriele Gühring. Unsupervised anomaly detection in multivariate time series with online evolving spiking neural networks. Machine Learning, 111(4):1377–1408, 2022.